

# Active chemo-mechanical solitons

L. Truskinovsky

PMMH, CNRS – UMR 7636, CNRS, ESPCI Paris, PSL Research University, 10 rue Vauquelin, 75005 Paris, France

G. Zurlo

School of Mathematical and Statistical Sciences, University of Galway, University Road, Galway, Ireland

In many biological systems localized mechanical information is transmitted by mechanically neutral chemical signals. Typical examples include contraction waves in acto-myosin cortex at cellular scale and peristaltic waves at tissue level. In such systems, chemical activity is transformed into mechanical deformation by distributed motor-type mechanisms represented by continuum degrees of freedom. To elucidate the underlying principles of chemo-mechanical coupling, we present in this Letter the simplest example. It involves directional motion of a localized solitary wave in a distributed mechanical system guided by a purely chemical cue. Our main result is that mechanical signals can be driven by chemical activity in a highly efficient manner.

While molecular biology and biochemistry clearly play dominant roles in biological processes, mechanics has recently emerged as another crucial co-player [1–4]. However, how chemically generated microscopic forces are transformed into a functional mechanical deformation at the macroscale still remains opaque [5, 6]. Of particular interest are the mechanisms of directional transmission of localized mechanical information by mechanically-neutral chemical signals. For instance, cardiac muscles have the ability to actively generate functional dynamic contractions [7], fluid propulsion of many cellular organisms is achieved by deformation waves [8, 9], fronts of cytoskeletal reinforcement were observed during epithelial monolayer expansion [10, 11] and finally peristalsis in digestive tract performs the most remarkable directed mechanical activity [12–14]. While the inner working of the corresponding chemical machinery can be modeled by various excitable reaction-diffusion systems [15], it remains unclear how a fueling chemical signal can transform into a propagating localized wave-like deformation field, and how such chemo-mechanical system can attain the observed high levels of energetic efficiency [16–19].

To elucidate the underlying principles of chemo-mechanical coupling we present in this Letter the simplest example of a directional motion of a solitary wave in a distributed mechanical system driven by a mechanically neutral signal of chemical origin. Such chemo-mechanical solitons (for simplicity) can be mechanically efficient only if the mechanical energy needed to activate the pulse at one edge is released due its closure at the other edge. As we show, such machinery can indeed be operative due to the existence of a mechanism of an internal energy transport through wave dispersion [20–22]. The mechanical signal can then propagate without taking any energy from the triggering chemical signal which implies an on board energy-harvesting.

To highlight ideas we consider in this Letter only a prototypical purely mechanical model of the corresponding dispersive mechanism without focusing on the underlying chemical machinery [23–26], and resorting to the simplest phenomenological approach in the description of active stress generation [27, 28]. Using such stylized framework, we show that a

mechanical solitary wave can be generated chemically even in a *linear* mechanical system. Moreover, we show that the chemo-mechanical coupling in such model is 100% efficient, which means that the active chemical system does not need to expend energy to sustain the mechanical signal beyond what is needed to maintain chemical activation.

Our main technical tool is the theory of dispersive systems allowing dynamical energy transport [29]. We build on the ideas developed in the theory of configurational defects in crystal lattices [30, 31], which can produce lattice scale energy radiation but can be also dynamically guided by lattice waves [31, 32]. Our goal is to show that the dispersion-induced mechanical turnover can ensure that the energy generated in sources is fully transmitted to sinks, making possible a loss-free propagation of mechanical information.

In the interest of analytical transparency, we consider only a 1D dynamic problem with  $u(x, t)$  denoting a scalar displacement field (longitudinal or transverse),  $x$  being a reference coordinate. Having in mind the elastic softness of the modeled biological prototypes, we assume that the system is elastically degenerate (infinitely stretchable), which brings into the theory a continuous symmetry. The corresponding Goldstone (soft) mode is described by the strain variable  $u_x$ , where the subscript indicates partial derivative. When the strain is a slowly varying inhomogeneous field, the corresponding small energy cost can be captured by a quadratic function of strain gradients, meaning that the implied infinitely soft material still carries gradient (bending) rigidity. The corresponding free energy is then  $\int \frac{\kappa}{2} u_{xx}^2 dx$  where  $\kappa$  is the bending modulus. Such energy emerges, for instance, in continuum representation of a deliberately minimalistic pantographic structure, as shown in Fig.1. It is built of inextensible but flexible beams, connected through ideal pivots. While the structure is floppy, showing zero stiffness when it is deformed uniformly[33], inhomogeneous deformations are energetically penalized due to nonzero bending rigidity of the beams [34]. More complex examples of bending-dominated structures can be found in the theory of high contrast elastic composites [35, 36]; in such systems the second order elasticity appears already at the leading order in the homogenization (continuum) limit, which justifies our

choice of the elastic energy.

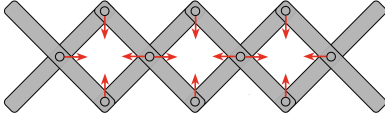


Figure 1: Mechanical model of pantograph with integrated active pulling (contractile) elements represented by red arrows.

In Fig. 1 we also show that the under-constrained pantograph structure can be stabilized through the pre-stress by active elements. To incorporate such elements into the model, we need to account for a term in the energy of the form  $\int \sigma_a(x, t) u_x dx$ . We further assume that the (pre)stress  $\sigma_a$  is piecewise constant spin variable taking three values  $\{\sigma_0, 0, -\sigma_0\}$ , intended to represent active stretching, deactivation and active compression, accordingly. In Fig.1 we illustrate the fact that all of these states can be achieved by using antagonistic, purely contractile elements; it also shows that contraction can be amplified by the arrangement which turns small microscopic deformations into large macroscopic movements [37].

To allow for dispersive non-dissipative energy transport in the model we also need to account for (pseudo)inertia by introducing into the energy the term  $\int \frac{\rho}{2} u_t^2 dx$ . The interpretation of such term as the actual kinetic energy may still make sense due to our choice of ultra-soft stretching elasticity, which turns into supersonic even for extremely slow mechanical signals. However, in physiological setting, the apparent mass density  $\rho$  should be rather viewed as bringing into the constitutive model an internal time scale, describing the functional, activity-induced, time delay. Such delay was found relevant, for instance, in the description of the activity of molecular motors, stretch receptors, ERK waves, etc. [10, 11, 38].

In view of the conservative nature of the mechanical part of the ensuing model, it will be convenient to obtain the corresponding dynamic equations and boundary conditions using Hamilton principle. The Lagrange function in our case has the form

$$L = \rho u_t^2 / 2 - \sigma_a(x, t) u_x - (\kappa/2) u_{xx}^2 \quad (1)$$

where the inhomogeneous controls  $\sigma_a(x, t)$  are assumed to be given. It will be also convenient to first rewrite the problem in more general terms by introducing the variables  $q^1 = x$  and  $q^2 = t$ , and presenting the displacement field in the form  $u(q^a)$ ,  $a = 1, 2$ . The corresponding action functional is

$$\mathcal{L} = \int_{\Omega} L(q^a, u_{,a}, u_{,ab}) dq^1 dq^2, \quad (2)$$

where we use subscripts after commas to indicate partial derivative, and where we introduced a two-dimensional *space-time* domain  $\Omega$  describing the evolution of a body between two time instants [39]. The corresponding Euler-Lagrange equations, representing the balance of linear momentum, take

the form  $(\delta L / \delta u_{,a})_{,a} = 0$ , where  $\delta L / \delta u_{,a} = \partial L / \partial u_{,a} - (\partial L / \partial u_{,ab})_{,b}$  is the variational derivative and the summation over repeated indexes is implied. In our special case we obtain the linear equation  $\rho u_{tt} = \sigma_x$  where  $\sigma = \sigma_a - \kappa u_{xxx}$ .

Suppose next that the domain  $\Omega$  contains a propagating surface  $\Sigma$  where the function  $\sigma_a(x, t)$  suffers a jump discontinuity, while it remains constant outside. On  $\Sigma$  the dependence of  $L$  on  $q^a$  is discontinuous, which leads to the possibility of energy sources or sinks. It is natural to assume that the particle trajectories on  $\Sigma$  are continuous, so that  $[[u]] = 0$ , where  $[[f]] = f^+ - f^-$  with the superscripts  $\pm$  denoting the limiting values of  $f$ . To ensure finiteness of the energy it is also natural to assume that the particle trajectories are smooth,  $[[u_x]] = 0$ . On  $\Sigma$  the stationarity of the action  $\mathcal{L}$  imposes the conditions representing continuity of tractions (forces) and hypertractions (moments) on the jump [40, 41]:  $[[\delta L / \delta u_{,a}]] n_a = 0$  and  $[[\delta L / \delta u_{,ab}]] n_a n_b = 0$ , where  $n_a$  is the unit vector normal to  $\Sigma$  facing the  $+$  direction. Note that mass balance on  $\Sigma$  is guaranteed by the kinematic compatibility condition  $[[u_{,a}]] = \mu n_a$ , where  $\mu$  is a scalar. The spatial  $n_x$  and temporal  $n_t$  components of the normal vector to  $\Sigma$  are related through  $n_t = -n_x D$ , where  $D$  is the normal velocity of the discontinuity, and we can always assume that  $n_x = 1$ . Eliminating  $\mu$  we obtain the relation  $D[[u_x]] + [[u_t]] = 0$ , requiring that on  $\Sigma$  not only the strain  $u_x$ , but also the velocity field  $u_t$  must be continuous.

Consider next a steadily propagating mechanical solitary wave (pulse) in the form of a traveling wave  $u(x, t) = u(z)$ , where  $z = x - Dt$  with  $D > 0$ . We assume that it is driven internally by a chemical signal also in the form of a traveling wave, generating a dynamic active stress distribution  $\sigma_a(x, t) = \sigma_a(z)$ . We further assume that the chemical activity wave can be represented by a combination of two mutually compensating rectangular pulses of compression and stretching:

$$\sigma_a(z) = \begin{cases} 0 & l < z & \text{(zone 1)} \\ -\sigma_0 & 0 < z < l & \text{(zone 2)} \\ \sigma_0 & -l < z < 0 & \text{(zone 3)} \\ 0 & z < -l & \text{(zone 4)} \end{cases} \quad (3)$$

where  $\sigma_0 > 0$  is the amplitude of chemical activity and  $2l$  is the size of the propagating activity zone, which so far is viewed as a parameter independent on  $D$ , the velocity of the traveling wave. We must therefore integrate the resulting linear equation in the four domains separated by the discontinuities of  $\sigma_a$ . Because the distribution of active stresses  $\sigma_a(z)$  is piecewise constant, it is equivalent to a set of localized self-equilibrated forces (couples) generating active compression in  $0 \leq z \leq l$  (zone 2) and active tension in  $-l \leq z \leq 0$  (zone 2).

The traveling wave solutions are found by solving a linear fourth order ODE with inhomogeneous right hand side:

$$\epsilon_{\text{eff}} u''(z) - \kappa u''''(z) = -\sigma'_a(z), \quad (4)$$

where  $u' = du/dz$  and  $\epsilon_{\text{eff}} = -\rho D^2 \leq 0$  is the effective tensile modulus; note that it is negative in our dynamically

dominated limit. On the moving surfaces of discontinuity of the active field  $\sigma_a(z)$  (points  $z = -l, 0, l$ ) the solutions to (4) should be matched using the corresponding jump conditions. When changing variables, the continuity conditions  $[[u]] = [[u_x]] = 0$  on the jumps become  $[[u]] = [[u']] = 0$ , whereas the continuity of tractions and hypertractions on the jumps gives  $[[\sigma_a - \kappa u''']] = 0$  and  $[[u''']] = 0$ . As we have already mentioned, on a surfaces  $\Sigma$  where the active stress  $\sigma_a(z)$  jumps, one can expect sources or sinks of energy. To find the rate of energy release (absorption) on such jump discontinuities, we need to assess the singular behavior on  $\Sigma$  of the energy momentum tensor [42, 43]

$$\tau_b^a = L \delta_b^a - u_{,b} \delta L / \delta u_{,a} - u_{,cb} \partial L / \partial u_{,ca}, \quad (5)$$

where  $\delta_b^a$  is the Kronecker symbol. Specifically, the temporal component of  $\tau_b^a$  controls the energy balance and if its normal projection

$$\mathcal{D} = [[\tau_2^a]] n_a \quad (6)$$

is nonzero on  $\Sigma$ , the latter is characterized by a nonzero singular energy release (absorption). In view of the imposed continuity conditions the rate of dissipation at every jump set is then

$$\mathcal{D} = D [[\sigma_a]] \{u_x\},$$

where  $\{f\} = (1/2)(f^+ + f^-)$ . It will be convenient to work with dimensionless variables and we set  $l_0 = \sqrt{\kappa/\sigma_0}$  and  $c_0 = \sqrt{\sigma_0/\rho}$  as the scales of length and velocity. The main nondimensional parameter of the problem is then

$$K = l/l_0.$$

In what follows we mark dimensionless variables with tildes, for instance,  $\tilde{z} = z/l_0$ ,  $\tilde{u} = u/l_0$ ,  $\tilde{D} = D/c_0$ . Then, our zone 1 corresponds to  $K \leq \tilde{z}$ , zone 2 to  $0 \leq \tilde{z} \leq K$ , zone 3 to  $-K \leq \tilde{z} \leq 0$ , and zone 4 to  $\tilde{z} \leq -K$ .

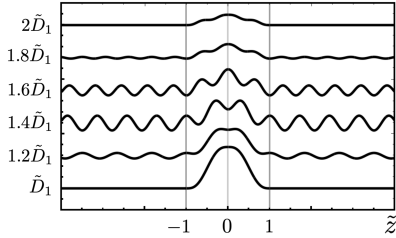


Figure 2: Solitary waves with periodic tails in the interval of driving velocities between  $\tilde{D}_1$  and  $\tilde{D}_2$ . Compact solitons constituting discrete spectrum (8) are represented by  $\tilde{D}_1$  and  $\tilde{D}_2 = 2\tilde{D}_1$ . Here  $K = 1$ .

In the case of interest the general solution of (4) has the form  $\tilde{u}_i(\tilde{z}) = c_{i1} + c_{i2}\tilde{z} + c_{i3} \cos(\tilde{D}\tilde{z}) + c_{i4} \sin(\tilde{D}\tilde{z})$ , where  $c_{ij}$  with  $i, j = 1, \dots, 4$  are integration constants in the four regions. In view of the possibility of oscillatory tails at  $\pm\infty$ , we can specify our *autonomous* solitary wave by imposing the boundary conditions  $\lim_{\tilde{z} \rightarrow \pm\infty} \lim_{\delta \rightarrow \infty} \frac{1}{\delta} \int_{\tilde{z}}^{\tilde{z}+\delta} u(\eta) d\eta = 0$ .

If we also impose the condition that singular sources and sinks of energy are absent, which means that  $\mathcal{D} = 0$  on all three singular boundaries, we obtain that

$$\tilde{u}_{1,4}(\tilde{z}) = \frac{1}{\tilde{D}^3} \cos((K \mp \tilde{z})\tilde{D}) \tan \frac{K\tilde{D}}{2}$$

in zones 1, 4, and

$$\tilde{u}_{2,3}(\tilde{z}) = \frac{1}{\tilde{D}^3} (\tilde{D}(\pm K - \tilde{z}) + \sin(\tilde{z}\tilde{D}) \mp \cos(\tilde{z}\tilde{D}) \tan \frac{K\tilde{D}}{2})$$

in zones 2, 3. The corresponding traveling wave solutions are illustrated in Fig. 2 for a range of values of velocities  $\tilde{D}$ .

Those of the obtained solutions which either receive energy from or radiate it towards  $\pm\infty$  would not be of interest for us. To obtain the energy balance equation in the bulk we can use Noether identity

$$(\tau_b^a)_{,a} = 0. \quad (7)$$

and then taking  $b = 2$ . In dimensional variables we obtain the equation

$$w_t + \mathcal{J}_x = 0,$$

where

$$w = \rho u_t^2/2 + \sigma_a u_x + (\kappa/2) u_{xx}^2$$

is the energy density and

$$\mathcal{J} = -\sigma u_t - \kappa u_{xt} u_{xx}$$

is the flux. If we now average the oscillatory part of the solution over the period we obtain  $\langle \mathcal{J} \rangle = D_g \langle w \rangle$  where  $\langle g \rangle = L^{-1} \int_0^L g(z) dz$  is the period averaging,  $L = 2\pi/k$ ,  $k = \tilde{D}/l_0$ . Here we also introduced the group velocity  $D_g = d\omega/dk$  where  $\omega = c_0 l_0 k^2$  is the corresponding dispersion relation. Note that in the traveling wave moving with velocity  $D$ , the emitted effective phonons are characterized by the condition that their phase velocity  $D_p = \omega/k = c_0 l_0 k$  is equal to the velocity of the pulse  $D_p = D$ . Note also that since in our case  $D_g/D_p = 2$  the solutions with oscillatory tails can harvest mechanical energy at  $-\infty$  and radiate it at  $+\infty$ .

If we now impose the condition that the average flux in the tails vanishes, we obtain that the corresponding pulses are necessarily *compact* with  $\tilde{u}_{1,4}(\tilde{z}) \equiv 0$ , and that such pulses exist only at discrete (quantized) values of velocity

$$\tilde{D}_n = 2n\pi/K, \quad (8)$$

where  $n = 0, 1, 2, \dots$ . This means, in particular, that narrow pulses move faster than the broad ones. Direct computation of the coefficients  $c_{ij}$  for such ‘‘compactons’’ in zones 2,3 gives

$$\tilde{u}_{2,3}(\tilde{z}) = (K/2n\pi)^2 (K \mp \tilde{z}) \pm (K/2n\pi)^3 \sin(2n\pi\tilde{z}/K)$$

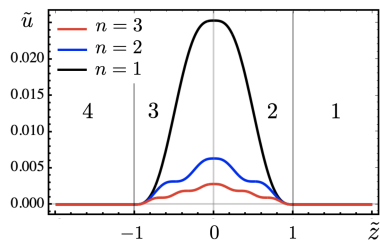


Figure 3: Dimensionless displacement in compactons for different values of  $n$ . Here  $K = 1$  and  $-2 \leq \tilde{z} \leq 2$ .

In Fig.3 we show the configuration of some pulses representing the discrete spectrum (8).

The presence of mechanical constrains on the spectrum of admissible velocities representing chemical signals suggests that there is a feedback between mechanical and chemical systems. In this sense, the constructed pulses are truly “chemo-mechanical” with inhomogeneity in the linear mechanical problem effectively representing non-linearity.

To understand better the energetics of the obtained solutions pulse propagation, we observe that for the steady propagation of the mechanical pulse it is necessary that around the internal boundary  $\tilde{z} = K$ , where the activity is switched on, energy is received. It is equally necessary that around the internal boundary  $\tilde{z} = -K$ , where the activity is turned off, energy is released. Note also that  $\mathcal{J}(z) = D_n w(z)$  so  $\mathcal{J}(z) \geq 0$  in regions 2 and 3 while  $\mathcal{J}(z) = 0$  in regions 1 and 4. Since  $D_g > D$ , the energy travels faster than the pulse itself and therefore there exists a relative unidirectional energy transfer from the back of the pulse to its front. In other words, the released mechanical energy at the rear of the pulse is exactly equal to the absorbed mechanical energy at the front of the pulse. One can then say that our system is harvesting the mechanical energy at one region and is relocating it with zero loss to another region. Therefore, while the chemical microscopic machinery expends energy to generate the pre-stress, no chemical energy is wasted to ensure the specifically mechanical performance of the system. In this sense the obtained pulses can be viewed as mechanically fully autonomous.

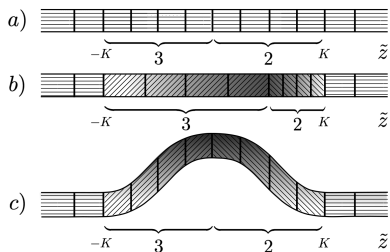


Figure 4: Schematic representation of a mechanical pulse advancing to the right. *a)* Reference (undeformed) configuration; *b)* deformed configuration in the case of longitudinal displacements; *c)* deformed configuration in the case of transverse displacements. The intensity of gray is proportional to the magnitude of displacement.

To clarify the physical meaning of the obtained solutions

it is instructive to focus on the pulse configuration with the largest amplitude, which corresponds to  $n = 1$ , and instead of perceiving it as representing dynamic longitudinal deformation, consider an equivalent case when a purely transverse deformation is driven by active shear, see Fig. 4. In this case we can think about a localized bulge (say, peristaltic “pump”) propagating along a dynamically pre-stressed beam placed without cohesion on a flat surface. The leading edge of such a bulge would then represent the tip of an opening “crack”, while the trailing edge would indicate the location of its closure (healing) side; the concept of such self-healing (autocatalytic) mechanical pulses is used, for instance, in modeling of earthquakes [44, 45]. In this context, the obtained solutions represent the case when energetically the cracking is exactly compensated by healing.

Another relevant analogy is with mechanical solitary waves in passive, nonlinear dispersive non-dissipative systems. Since the corresponding localized wave packets are energy conserving, they also necessarily support an internal energy transfer between the leading and the trailing segments. For instance, in the case of discrete FPU-type solitons, one can interpret the leading edge as a partially developed *admissible* shock wave while the trailing segment can be similarly viewed as a *non-admissible* shock wave [46]. In this case the nature of dispersion is different and the energy transport takes place from the front to the back so that the “dissipative” shock “feeds” (and in this way stabilizes) the “anti-dissipative” one [21, 47].

To conclude, we developed a prototypical model of a chemo-mechanical soliton driven by a passive-to-active transformation at the front and a matching active-to-passive transformation at the rear. We showed that such solitons can be generated by dynamic inhomogeneities even in the simplest *linear* mechanical systems. The obtained solutions can be interpreted as describing spatially distributed chemo-mechanical motors converting mechanically neutral chemical signals into functional mechanical activity. There is a considerable interest to reproduce such biological mechanisms artificially in soft robots [48–51], and in this sense the proposed model can serve as a proof of concept. Future work aimed at fully quantitative designs should also account for dissipation (friction) and functional work (cargo) as well as being set in a realistic 3D geometry.

*Acknowledgments.* The authors thank P. Recho, A. Vainchtein, G. Mishuris and N. Gorbushin for helpful discussions. L.T. acknowledges the support under the grants ANR-17-CE08-0047-02 and ANR-21-CE08-MESOCRYSP.

- [1] T. Savin, N. A. Kurpios, A. E. Shyer, P. Florescu, H. Liang, L. Mahadevan, and C. J. Tabin, On the growth and form of the gut, *Nature* **476**, 57 (2011).
- [2] E. Coen and D. J. Cosgrove, The mechanics of plant morphogenesis, *Science* **379**, eade8055 (2023).
- [3] P. Lappalainen, T. Kotila, A. Jégou, and G. Romet-Lemonne,

- Biochemical and mechanical regulation of actin dynamics, *Nature Reviews Molecular Cell Biology* **23**, 836 (2022).
- [4] L. Truskinovsky, G. Vitale, and T. Smit, A mechanical perspective on vertebral segmentation, *International Journal of Engineering Science* **83**, 124 (2014).
- [5] B. Slater, W. Jung, and T. Kim, Emergence of diverse patterns driven by molecular motors in the motility assay, *Cytoskeleton* (2023).
- [6] B. Wang and Y. Lu, Collective molecular machines: Multidimensionality and reconfigurability, *Nano-Micro Letters* **16**, 155 (2024).
- [7] C. R. Bagshaw, *Muscle contraction* (Springer Science & Business Media, 1993).
- [8] C. B. Lindemann and K. A. Lesich, The mechanics of cilia and flagella: What we know and what we need to know, *Cytoskeleton* (2024).
- [9] M. Beeby, J. L. Ferreira, P. Tripp, S.-V. Albers, and D. R. Mitchell, Propulsive nanomachines: the convergent evolution of archaella, flagella and cilia, *FEMS microbiology reviews* **44**, 253 (2020).
- [10] X. Serra-Picamal, V. Conte, R. Vincent, E. Anon, D. T. Tambe, E. Bazellieres, J. P. Butler, J. J. Fredberg, and X. Trepat, Mechanical waves during tissue expansion, *Nature Physics* **8**, 628 (2012).
- [11] D. Boockch, N. Hino, N. Ruzickova, T. Hirashima, and E. Hannezo, Theory of mechanochemical patterning and optimal migration in cell monolayers, *Nature physics* **17**, 267 (2021).
- [12] M. D. Sinnott, P. W. Cleary, and S. M. Harrison, Peristaltic transport of a particulate suspension in the small intestine, *Applied Mathematical Modelling* **44**, 143 (2017).
- [13] K. J. Quillin, Kinematic scaling of locomotion by hydrostatic animals: ontogeny of peristaltic crawling by the earthworm *lumbicus terrestris*, *Journal of Experimental Biology* **202**, 661 (1999).
- [14] N. Gorbushin and L. Truskinovsky, Peristalsis by pulses of activity, *Physical Review E* **103**, 042411 (2021).
- [15] L. M. Pismen, *Patterns and interfaces in dissipative dynamics*, Vol. 706 (Springer, 2006).
- [16] F. Pérez-Verdugo, S. Banks, and S. Banerjee, Excitable dynamics driven by mechanical feedback in biological tissues, *Communications Physics* **7**, 167 (2024).
- [17] A. Kindberg, J. K. Hu, and J. O. Bush, Forced to communicate: Integration of mechanical and biochemical signaling in morphogenesis, *Current opinion in cell biology* **66**, 59 (2020).
- [18] F. Alisafaei, X. Chen, T. Leahy, P. A. Janmey, and V. B. Shenoy, Long-range mechanical signaling in biological systems, *Soft matter* **17**, 241 (2021).
- [19] D. Dean, A. S. Nain, and G. M. Genin, *Mechanics of cells and fibers* (2023).
- [20] Y. V. Kartashov, B. A. Malomed, and L. Torner, Solitons in nonlinear lattices, *Reviews of Modern Physics* **83**, 247 (2011).
- [21] L. Truskinovsky and A. Vainchtein, Solitary waves in a nonintegrable fermi-pasta-ulam chain, *Physical Review E* **90**, 042903 (2014).
- [22] Y. Ming, L. Ye, H.-S. Chen, S.-F. Mao, H.-M. Li, and Z.-J. Ding, Solitons as candidates for energy carriers in fermi-pasta-ulam lattices, *Physical Review E* **97**, 012221 (2018).
- [23] O. Dudchenko and G. T. Guria, Self-sustained peristaltic waves: explicit asymptotic solutions, *Physical Review E, Statistical, Nonlinear, and Soft Matter Physics* **85**, 020902 (2012).
- [24] D. Ambrosi and S. Pezzuto, Active stress vs. active strain in mechanobiology: constitutive issues, *Journal of Elasticity* **107**, 199 (2012).
- [25] E. Brunello and L. Fusi, Regulating striated muscle contraction: Through thick and thin, *Annual Review of Physiology* **86**, 255 (2024).
- [26] M. Caruel and L. Truskinovsky, Physics of muscle contraction, *Reports on Progress in Physics* **81**, 036602 (2018).
- [27] J. Prost, F. Jülicher, and J.-F. Joanny, Active gel physics, *Nature physics* **11**, 111 (2015).
- [28] K. Kruse, J.-F. Joanny, F. Jülicher, J. Prost, and K. Sekimoto, Generic theory of active polar gels: a paradigm for cytoskeletal dynamics, *The European Physical Journal E* **16**, 5 (2005).
- [29] G. B. Whitham, *Linear and nonlinear waves* (John Wiley & Sons, 2011).
- [30] O. Kresse and L. Truskinovsky, Lattice friction for crystalline defects: from dislocations to cracks, *Journal of the Mechanics and Physics of Solids* **52**, 2521 (2004).
- [31] L. I. Slepyan, *Models and phenomena in fracture mechanics* (Springer Science & Business Media, 2012).
- [32] N. Gorbushin, G. Mishuris, and L. Truskinovsky, Frictionless motion of lattice defects, *Physical Review Letters* **125**, 195502 (2020).
- [33] M. Schenk and S. D. Guest, On zero stiffness, *Proceedings of the Institution of Mechanical Engineers, Part C: Journal of Mechanical Engineering Science* **228**, 1701 (2014).
- [34] J.-J. Alibert, P. Seppecher, and F. Dell'Isola, Truss modular beams with deformation energy depending on higher displacement gradients, *Mathematics and Mechanics of Solids* **8**, 51 (2003).
- [35] C. Boutin, J. Soubestre, M. S. Dietz, and C. Taylor, Experimental evidence of the high-gradient behaviour of fiber reinforced materials, *European Journal of Mechanics-A/Solids* **42**, 280 (2013).
- [36] M. Camar-Eddine and P. Seppecher, Determination of the closure of the set of elasticity functionals, *Archive for rational mechanics and analysis* **170**, 211 (2003).
- [37] L. Mahadevan and P. Matsudaira, Motility powered by supramolecular springs and ratchets, *Science* **288**, 95 (2000).
- [38] M. Badoual, F. Jülicher, and J. Prost, Bidirectional cooperative motion of molecular motors, *Proceedings of the National Academy of Sciences* **99**, 6696 (2002).
- [39] S. Gavriluk, B. Nkonga, K.-M. Shyue, and L. Truskinovsky, Stationary shock-like transition fronts in dispersive systems, *Nonlinearity* **33**, 5477 (2020).
- [40] R. D. Mindlin and H. Tiersten, Effects of couple-stresses in linear elasticity, *Archive for Rational Mechanics and analysis* **11**, 415 (1962).
- [41] R. A. Toupin, Theories of elasticity with couple-stress, *Archive for Rational Mechanics and Analysis* **17**, 85 (1964).
- [42] J. Eshelby, The elastic energy-momentum tensor, *Journal of elasticity* **5**, 321 (1975).
- [43] L. Truskinovskii, Dynamics of non-equilibrium phase boundaries in a heat conducting non-linearly elastic medium, *Journal of Applied Mathematics and Mechanics* **51**, 777 (1987).
- [44] G. Perrin, J. R. Rice, and G. Zheng, Self-healing slip pulse on a frictional surface, *Journal of the Mechanics and Physics of Solids* **43**, 1461 (1995).
- [45] K. Thøgersen, E. Aharonov, F. Barras, and F. Renard, Minimal model for the onset of slip pulses in frictional rupture, *Physical Review E* **103**, 052802 (2021).
- [46] C. M. Dafermos, *Hyperbolic conservation laws in continuum physics*, Vol. 3 (Springer, 2005).
- [47] A. Vainchtein and L. Truskinovsky, Solitary waves and kinks in fpu lattices with soft-hard-soft trilinear interactions, *arXiv preprint arXiv:2405.09302* (2024).
- [48] D. Agostinelli, F. Alouges, and A. DeSimone, Peristaltic waves as optimal gaits in metameric bio-inspired robots, *Frontiers in*

- Robotics and AI **5**, 99 (2018).
- [49] P. W. Miller and J. Dunkel, Gait-optimized locomotion of wave-driven soft sheets, *Soft Matter* **16**, 3991 (2020).
- [50] C. Pehlevan, P. Paoletti, and L. Mahadevan, Integrative neuromechanics of crawling in *d. melanogaster* larvae, *Elife* **5**, e11031 (2016).
- [51] P. Recho and L. Truskinovsky, Optimal crawling: from mechanical to chemical actuation, arXiv preprint arXiv:2406.06437 (2024).